Supporting Information

Ag-Si artificial microflowers for plasmon-enhanced solar water splitting

Chih-Jung Chen,[a] Ming-Guei Chen,[b] Chih Kai Chen,[a] Pin Chieh Wu,[c] Po-Tzu Chen,[c] Mrinmoyee Basu,[a] Shu-Fen Hu,*[b] Din Ping Tsai[c] and Ru-Shi Liu*[ad]

[a] Department of Chemistry, National Taiwan University, Taipei 106, Taiwan. Email:
[b] Department of Physics, National Taiwan Normal University, Taipei 116, Taiwan.
[c] Graduate Institute of Applied Physics, National Taiwan University Taipei 106, Taiwan and Research Center for Applied Sciences, Academia Sinica, Taipei 115, Taiwan.
[d] Department of Mechanical Engineering and Graduate Institute of Manufacturing Technology, National Taipei University of Technology, Taipei 106, Taiwan

* Email: sfhu.hu@ntnu.edu.tw Fax:+886-2-29326408; Tel: +886-2-77346079 and rsliu@ntu.edu.tw Fax:+886-2-33668671; Tel: +886-2-33661169

Experimental Section

Fabrication of Si MW array. Figure S1 shows the fabrication procedure of the Si MW array. Boron-doped p-type (110)-oriented Si wafers (resistivity: 1~15Ω cm) were cleaned using RCA procedure. Wet oxide with 500 nm thickness was grown on the Si surface through a low-pressure chemical vapor deposition (LPCVD) system. An 800 nm thick photoresist layer was spin-coated on the oxide and then exposed to develop a square array with 1.7 μm pitch size. The SiO_2 exposed through the holes of the photoresist layer was etched using Ar plasma under CF_4 and CHF_3 atmosphere to reveal the underlying Si substrate. The photoresist square array was subsequently removed using O_2 plasma at 250°C for 30 s and immersed into a H_2SO_4 solution at 120°C for 10 min to eliminate the residual photoresist square array. The 1 and 3 μm long Si MW arrays were etched using a transformer coupled plasma (TCP) etching technology under Cl_2 and HBr atmosphere with various etching time. Meanwhile, the 12 μm long Si MW array was fabricated using ICP-RIE fabrication at 110°C under SF_6 and O_2 atmosphere. After dry etching process,

all Si MW arrays were immersed in diluted HF acid solution for 60 s to remove the SiO_2 hard masks. The back side of the Si MW array was polished to 350 μm thickness and deposited on Al back electrode with 500 nm thickness by an E-gun evaporator system.

Preparation of Ag-Si photocathode. Cu wire was mounted on the Al back electrode of the as-prepared Si MW array using Ag paste and was fixed with an insulating epoxy. The native oxide of the Si MW electrodes was etched with diluted HF acid solution for 30 s and subsequently immersed in a mixed aqueous solution of 5 M HF acid and 5 mM $AgNO_3$ for a desired duration to deposit Ag particles. Here, the insulating epoxy functions as a mask to prevent the Al back electrode from being etched by the mixed solution. Moreover, Figure S6f shows that there was no Ag particle attaching on the bottom part of Ag-Si electrode through this facile decorating method. For comparison, Pt-Si electrodes were fabricated by same procedure. The only difference was the reacting agent prepared through mixing 5 M HF acid and 5 mM H_2PtCl_6. The Pt-Si electrode was abbreviated to "Pt-Si-T", in which T represents deposition time. Figure S11d-e presents the Pt particles aggregated on the tips of Si MWs. Here, we also uniformly modified Ag particles on Si MWs through thermal reduction. The 3 μmL of 1 mM $AgNO_3$ dissolved in absolute ethanol was dropped on Si MWs and heated through rapid thermal annealing (RTA) system. This step was repeated to increase the Ag loading amount. The $AgNO_3$ coated-Si MWs was then reduced under 5% H_2 + Ar atmosphere at 500°C for 1 h in the tube furnace. The uniformly Ag decorated-Si electrode was abbreviated to "Ag╳S", in which S represents times of coating steps. Figure S11a-c shows the Ag particles uniformly attached on whole Si MWs.

Photoelectrochemical Measurement. Photoelectrochemical characterization was performed in a three-electrode system. The electrolyte of PEC cell consisted of 0.5 M Na_2SO_4 aqueous solution (250 mL) at pH = 1, which was tuned by the concentrated H_2SO_4. The three-electrode configuration was composed of an Ag-Si MW array, Pt foil, and Ag/AgCl electrode as the working, counter, and reference electrodes, respectively. The PEC cell was illuminated with a xenon lamp equipped with AM 1.5 filter, and the light intensity was fixed at 100 mW/cm^2. All PEC data was recorded using a potentiostat (Eco Chemie AUTOLAB, The Netherlands) and GPES (General Purpose Electrochemical System) software at 25°C. A linear-sweep voltammogram of Ag-Si photocathode was obtained from 0 V to -1.0 V with a scan rate of 20 mV/s. The chronoamperometry, gas evolution and IPCE were characterized under an applied bias of -1.0 V. The areas of photoelectrodes for gas evolution were the same as those were characterized of photocurrent. The EIS data was measured by an electrochemical workstation (760D, CH Instruments) under an applied bias of -0.18 V (vs Ag/AgCl), which was corresponded to the on-set potential (defined as the current reaching -1.0 mA/cm^2), under various wavelengths of irradiation. The sweeping frequency was conducted from 350 kHz to 0.1 Hz with a 10 mV amplitude.

Characterization of Materials. The morphologies of the Ag-Si microflowers were investigated using a JEOL JSM-6700F field-emission SEM. A series of UV-Vis absorption spectra of the Ag-Si photocathodes were characterized

using the Thermo EVOLUTION 220 spectrometer. A Bruker D2 PHASER XRD analyzer with Cu Kα radiation (λ = 1.54178 Å) was utilized to obtain crystallographic information on the Si MW array. The Raman spectra of the Si MW array were elucidated using a Thermo DXR microscope with a 532 nm laser. The XPS spectra of the photoelectrodes were performed through a PHI Quantera surface analysis equipment with Al Kα radiation (λ = 8.3406 Å).

FEM Simulation. All of the simulation spectra and electromagnetic field distributions were obtained by solving the three-dimensional Maxwell equations through the commercial COMSOL Multiphysics software. To study the Si microwire array, the periodic boundary condition was used for the unit cell. The refractive index of Si was retrieved from the SOPRA N&K Database. The permittivity of Ag under UV-Vis radiation was described by the Drude-Lorentz model. To reveal the surface plasmon excitation of the Ag nanostructures at specific wavelengths, all simulation modules with *y*-polarized illumination were established according to the SEM images. By calculating the scattering parameters (S-parameters), we obtained the absorbance spectrum expressed by $A = 1 - R - T$, where R is reflectance and T is transmittance.

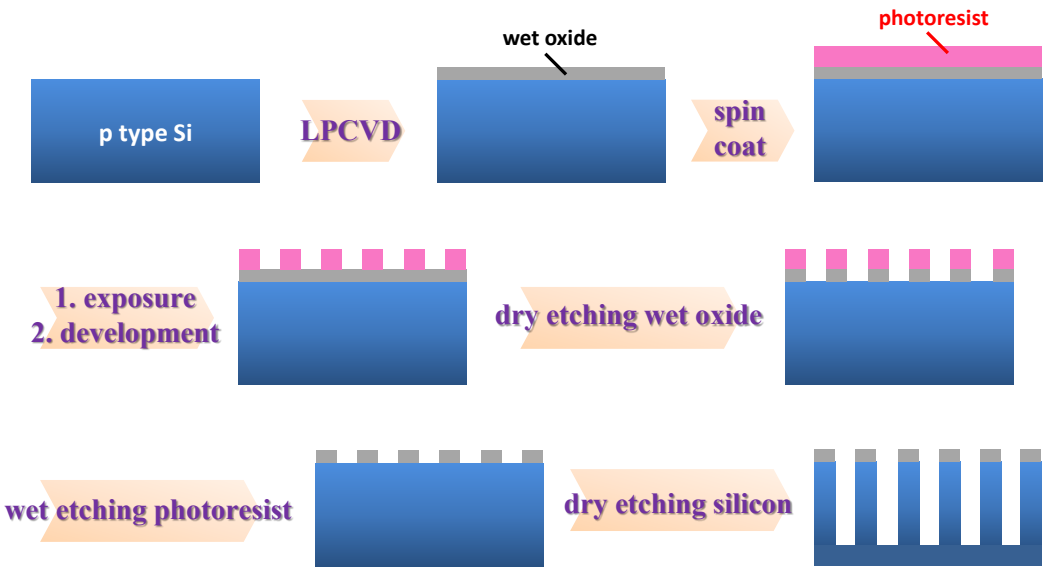

Figure S1. Fabrication procedure of Si MW array.

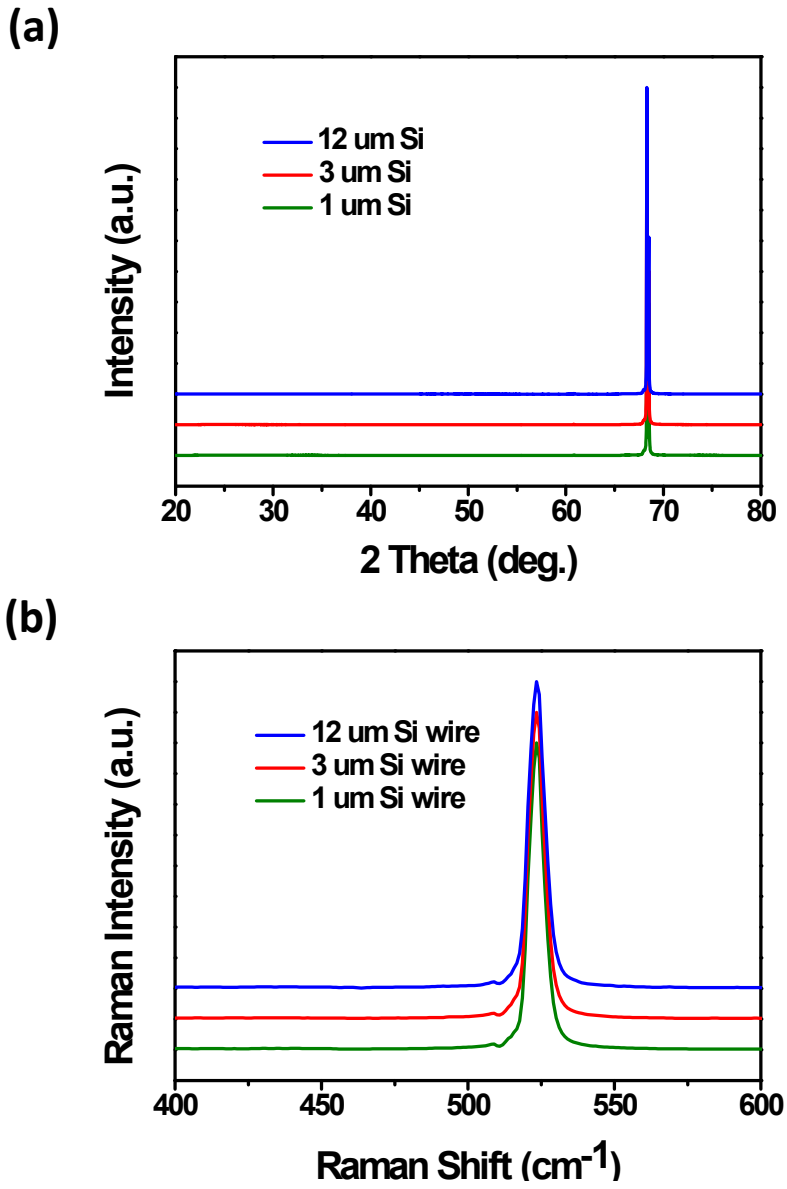

Figure S2. (a) XRD and (b) Raman spectra of Si MW arrays with various lengths.

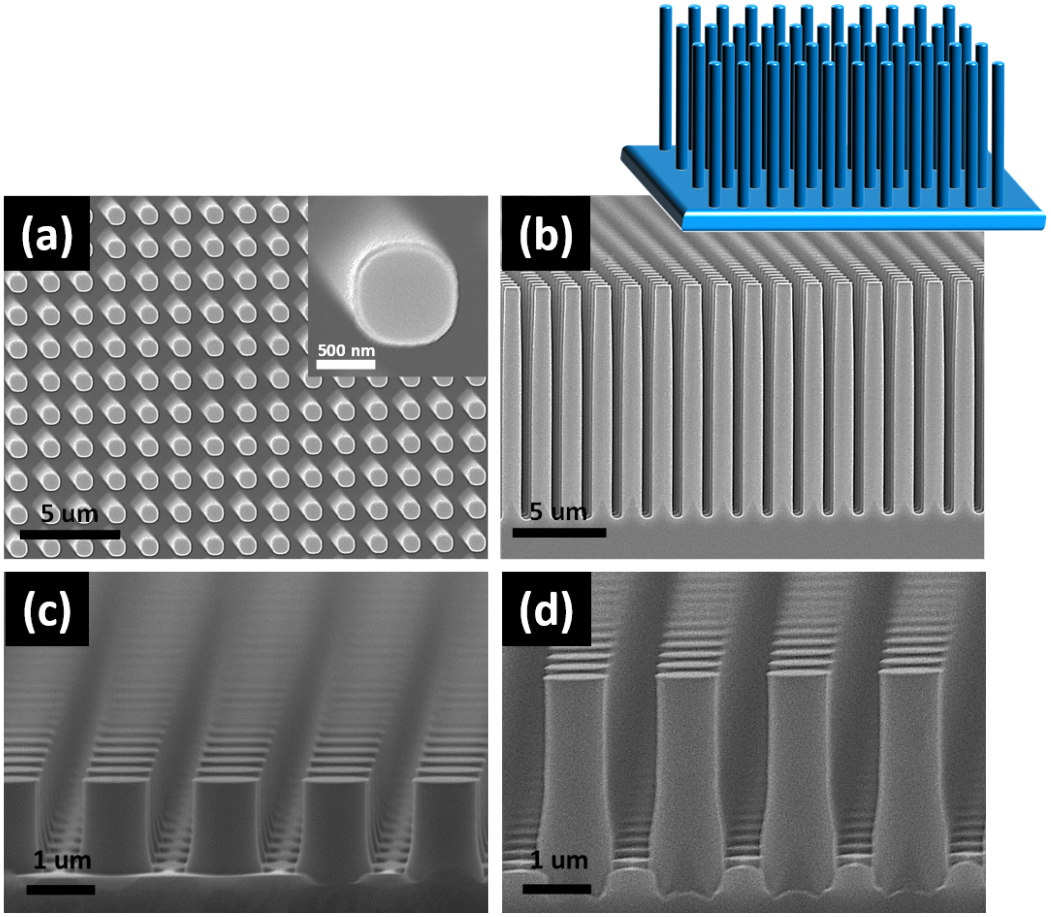

Figure S3. (a) Top view SEM image of Si MW array with 12 μm length. Cross-sectional SEM images of Si MW array with (b) 12 μm, (c) 1 μm, and (d) 3 μm lengths.

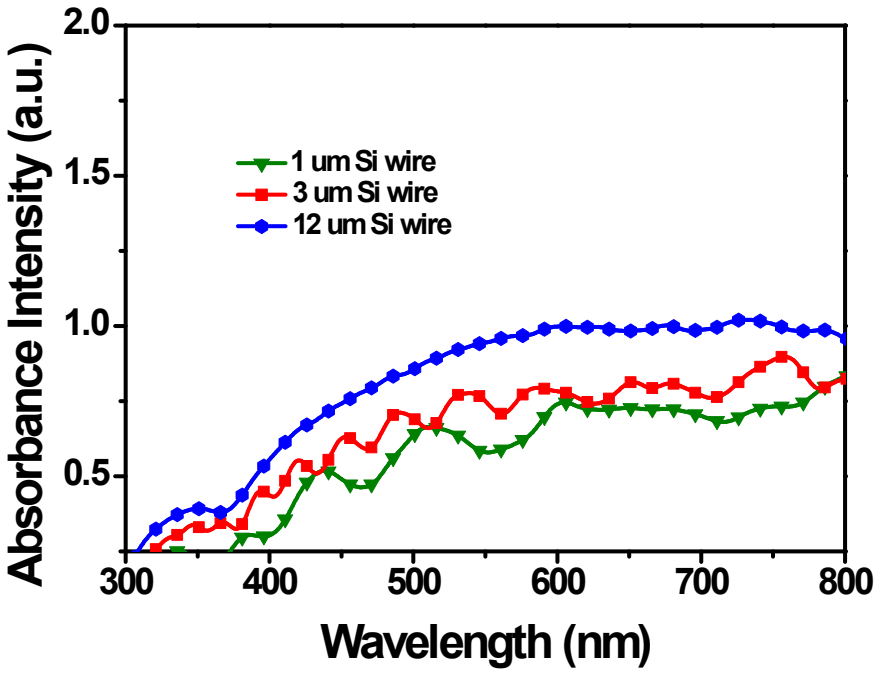

Figure S4. UV-Vis absorption spectrum of Si MW arrays with various lengths.

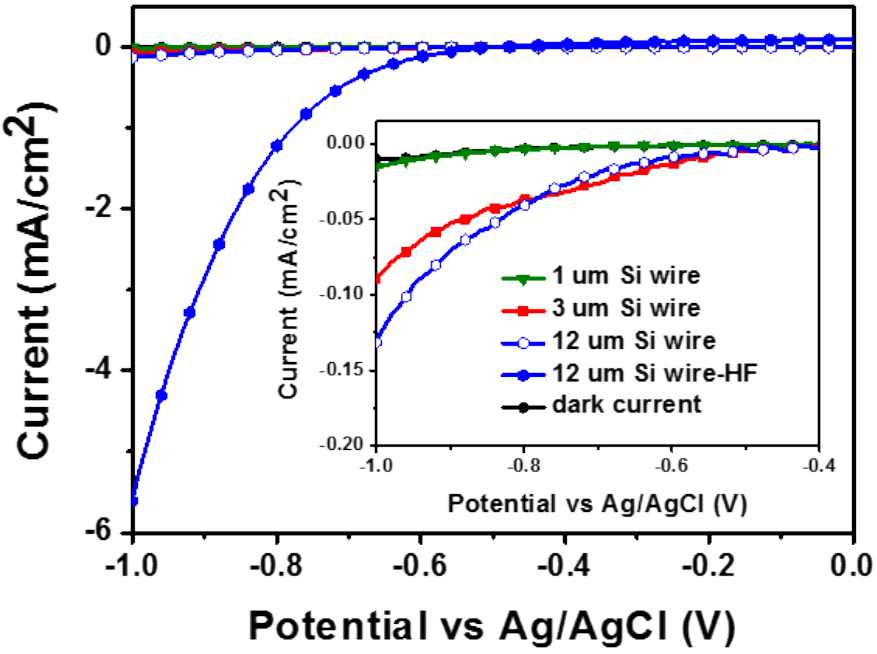

Figure S5. Linear-sweep voltammograms of Si MW arrays with various lengths.

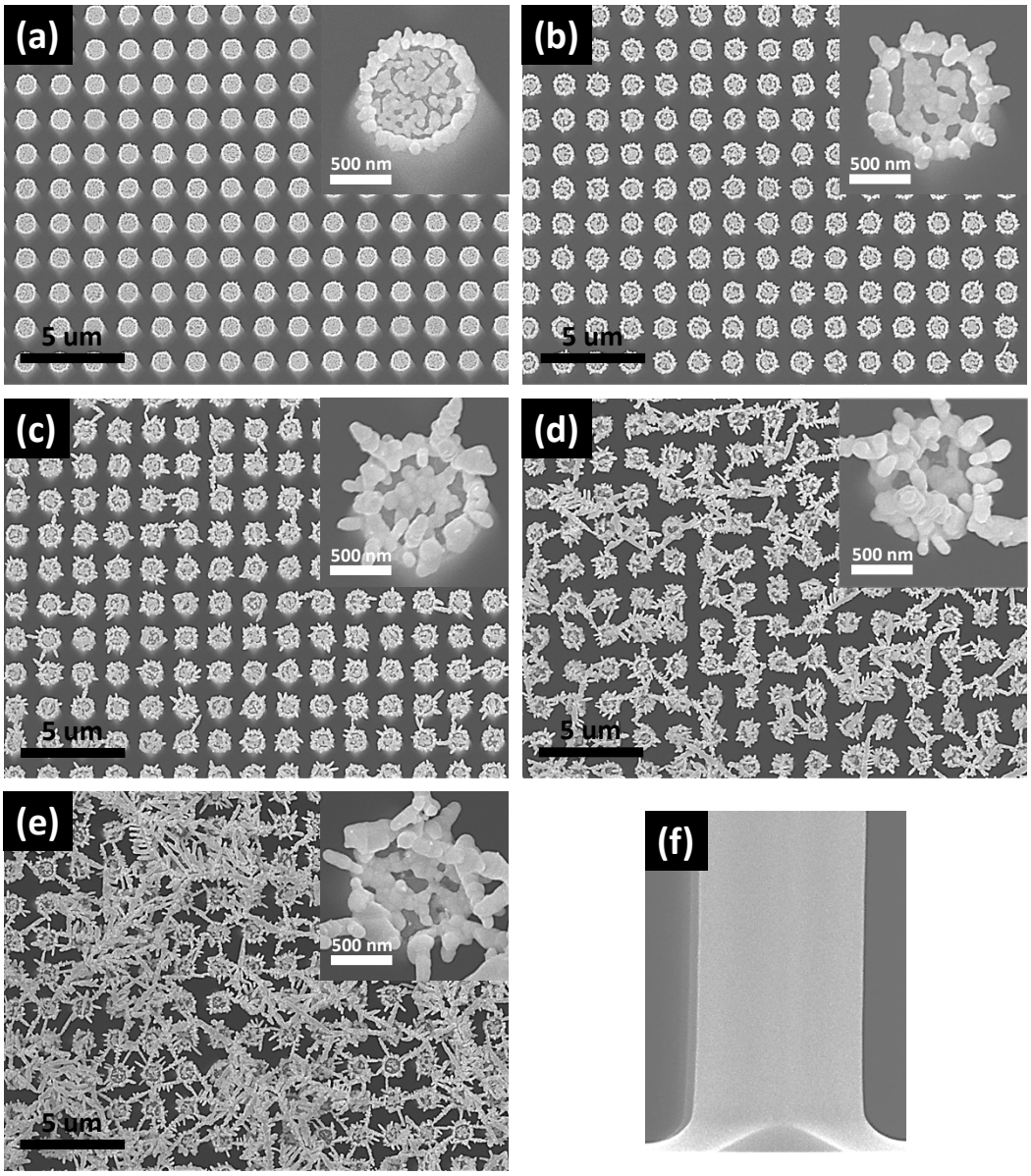

Figure S6. Top view SEM images of Ag-Si MW array with (a) 10, (b) 20, (c) 40, (d) 60, and (e) 90 s deposition time. (f) Cross-sectional SEM image focused on the bottom part of Ag-Si electrode.

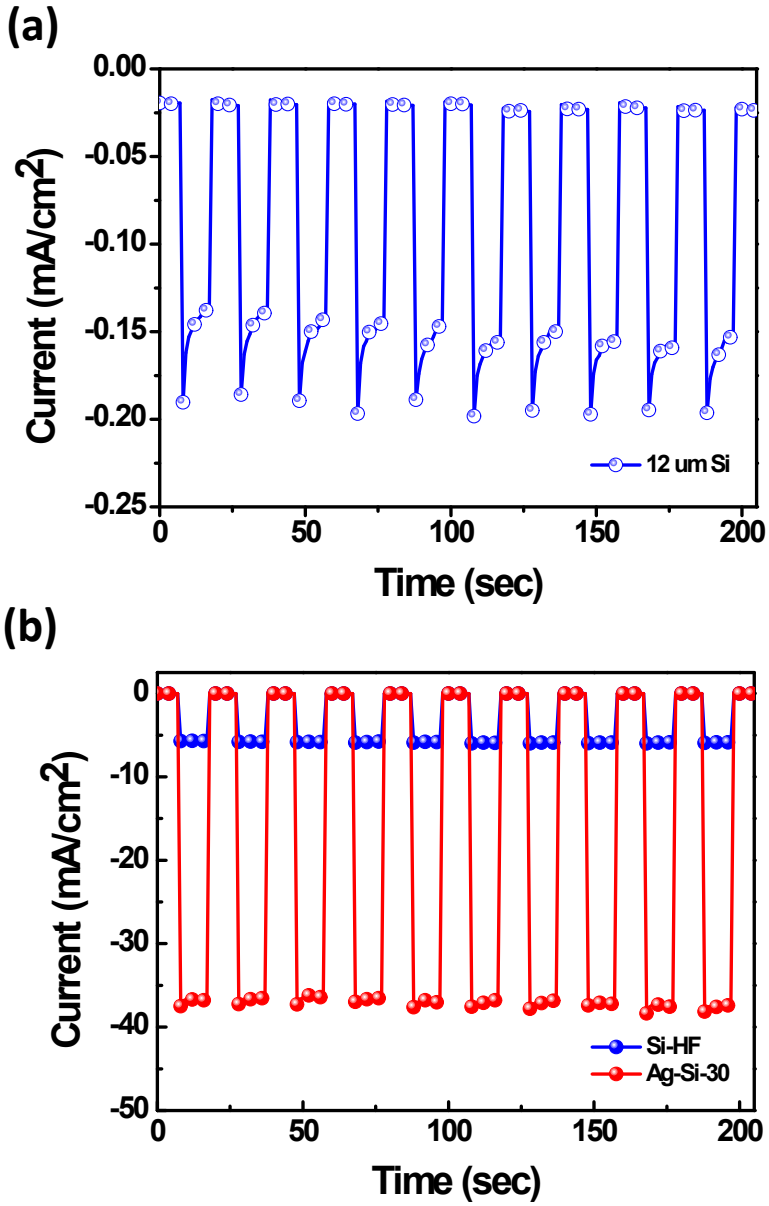

Figure S7. Transient photocurrent density of (a) pristine Si, (b) Si-HF and Ag-Si electrode with 30 sec deposition at -1.0 V (vs. Ag/AgCl).

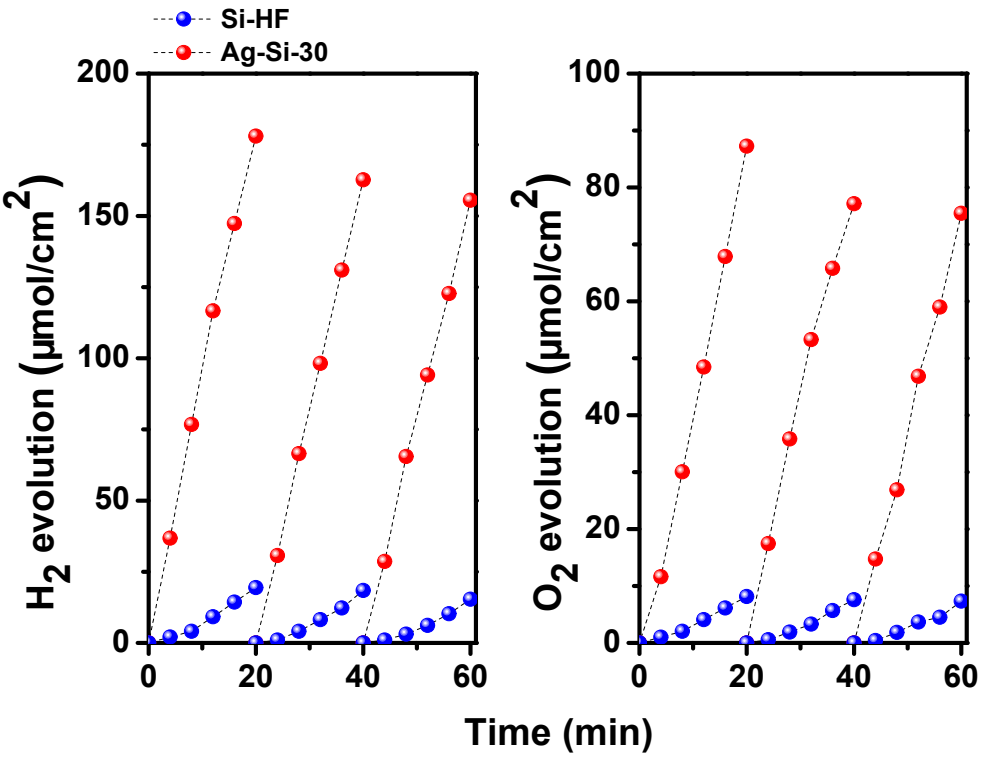

Figure S8. Gas evolution of pristine Si and Ag-Si electrode with 30 sec deposition at -1.0 V (vs. Ag/AgCl).

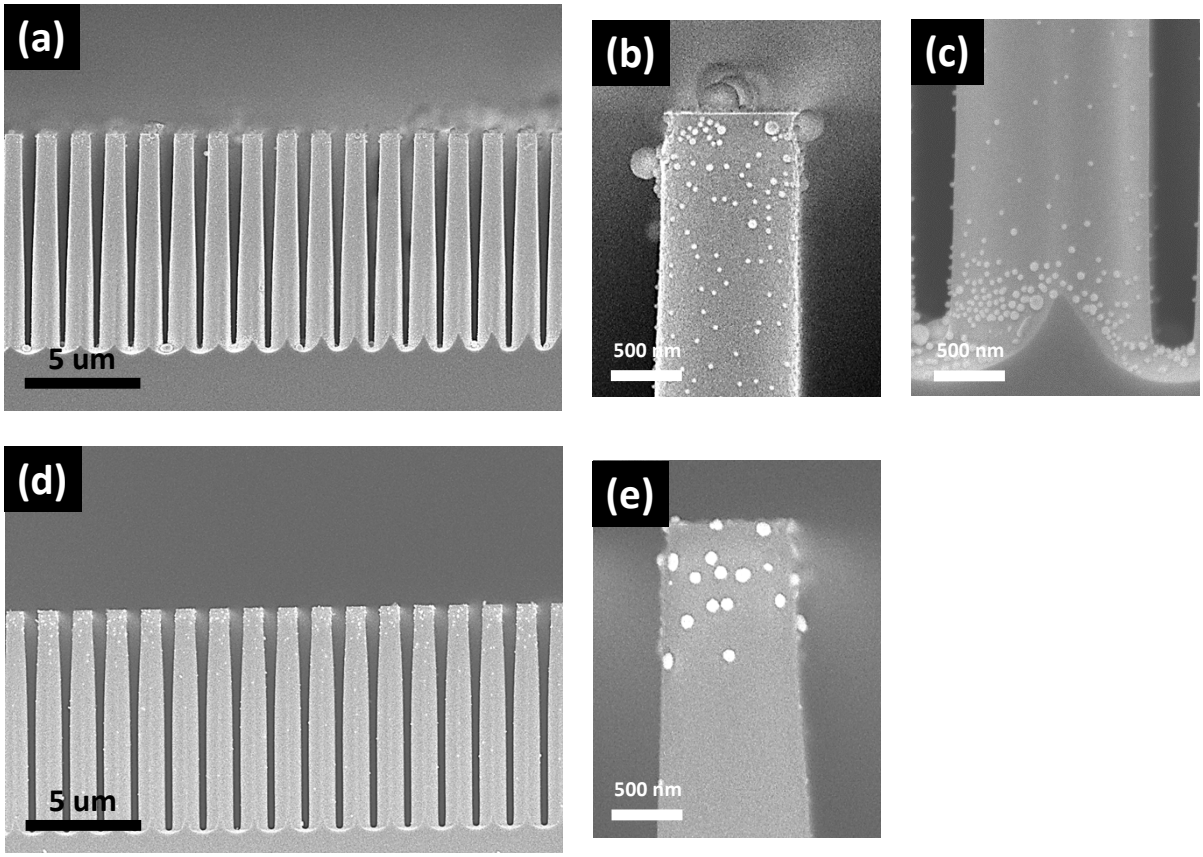

Figure S9. Cross-sectional SEM images of (a-c) Ag uniformly decorated-Si MWs and (d-e) Pt partially decorated-Si MWs

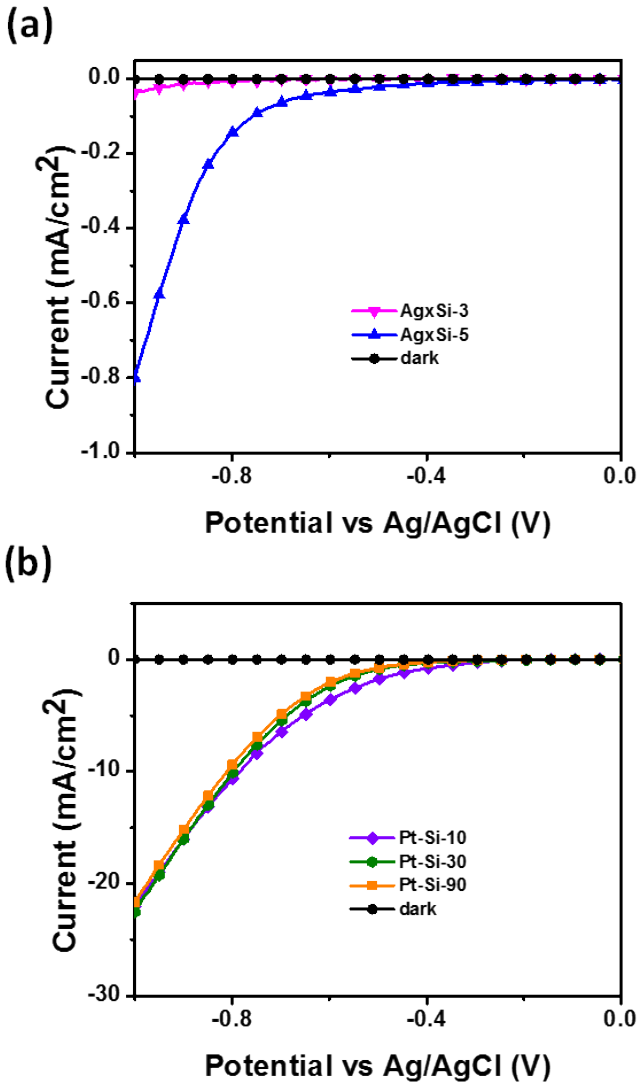

Figure S10. Linear-sweep voltammograms of (a) Ag uniformly decorated-Si MWs and (b) Pt partially decorated-Si MWs with different loading amounts.

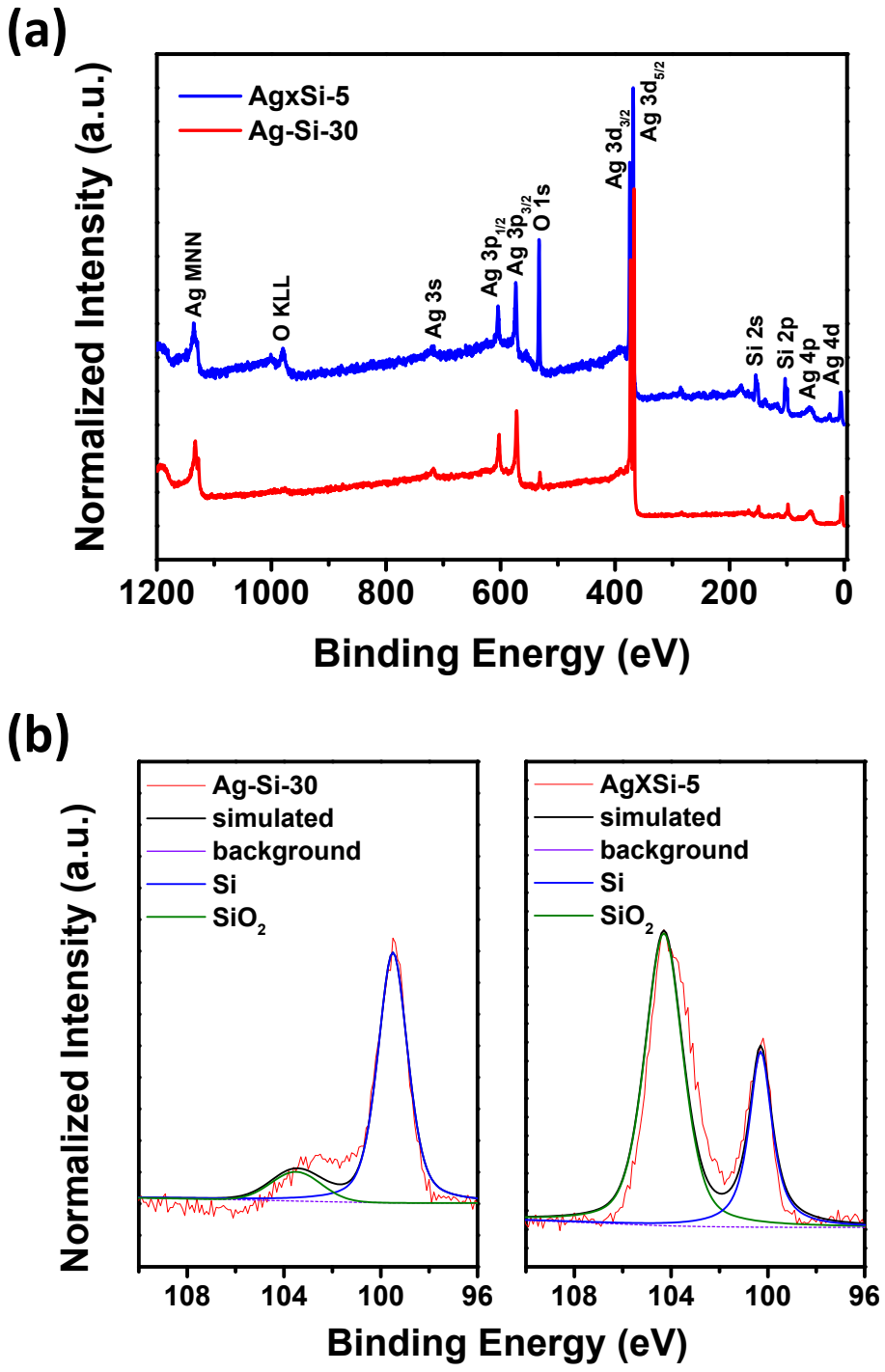

Figure S11. (a) XPS spectrum and (b) high-resolution Si 2p XPS spectra of Ag-Si-30 and Ag╳S-5 photocathodes.

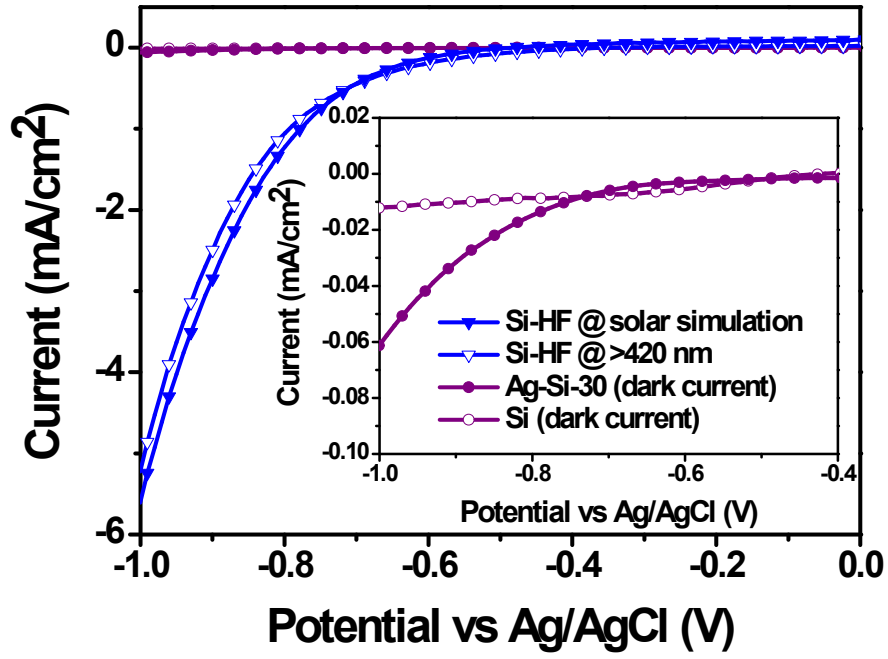

Figure S12. Linear-sweep voltammograms of Si MW arrays with various lengths.

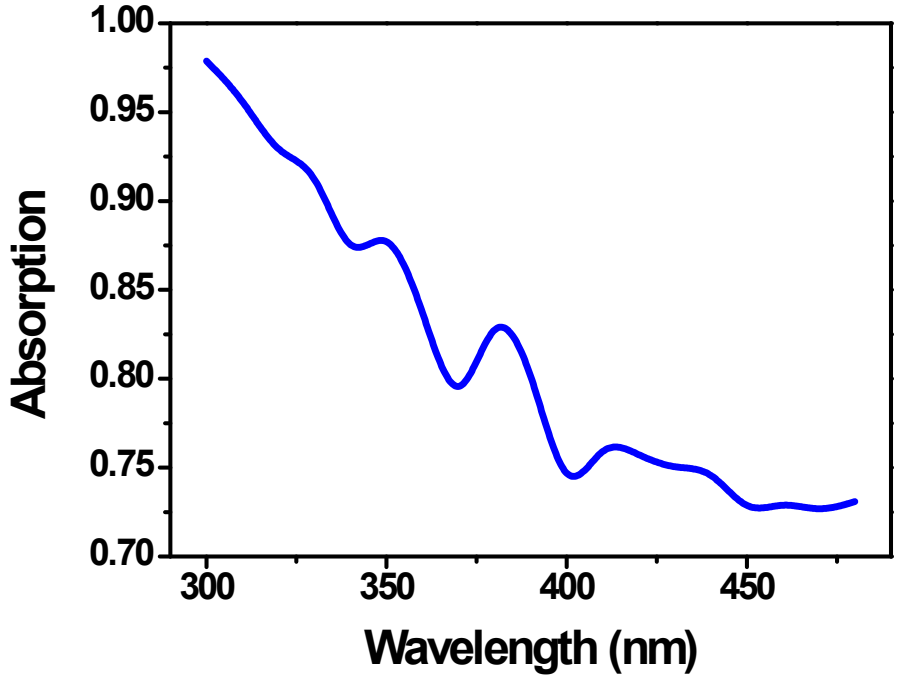

Figure S13. Absorption spectrum of Ag-deposited Si MW array from FEM simulations.

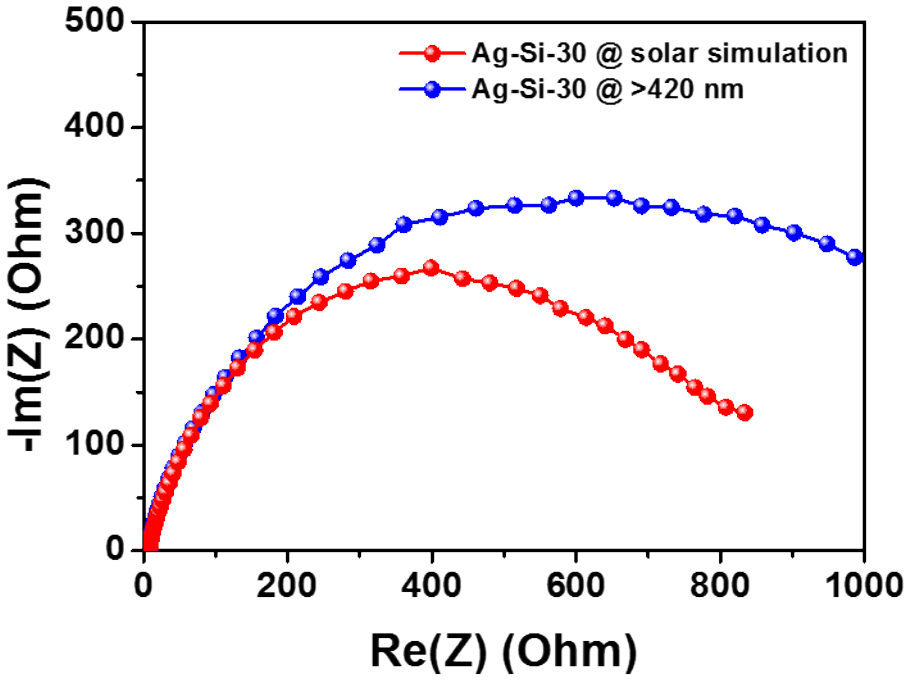

Figure S14. EIS of Ag-Si electrode with 30 s deposition under various wavelengths irradiation.

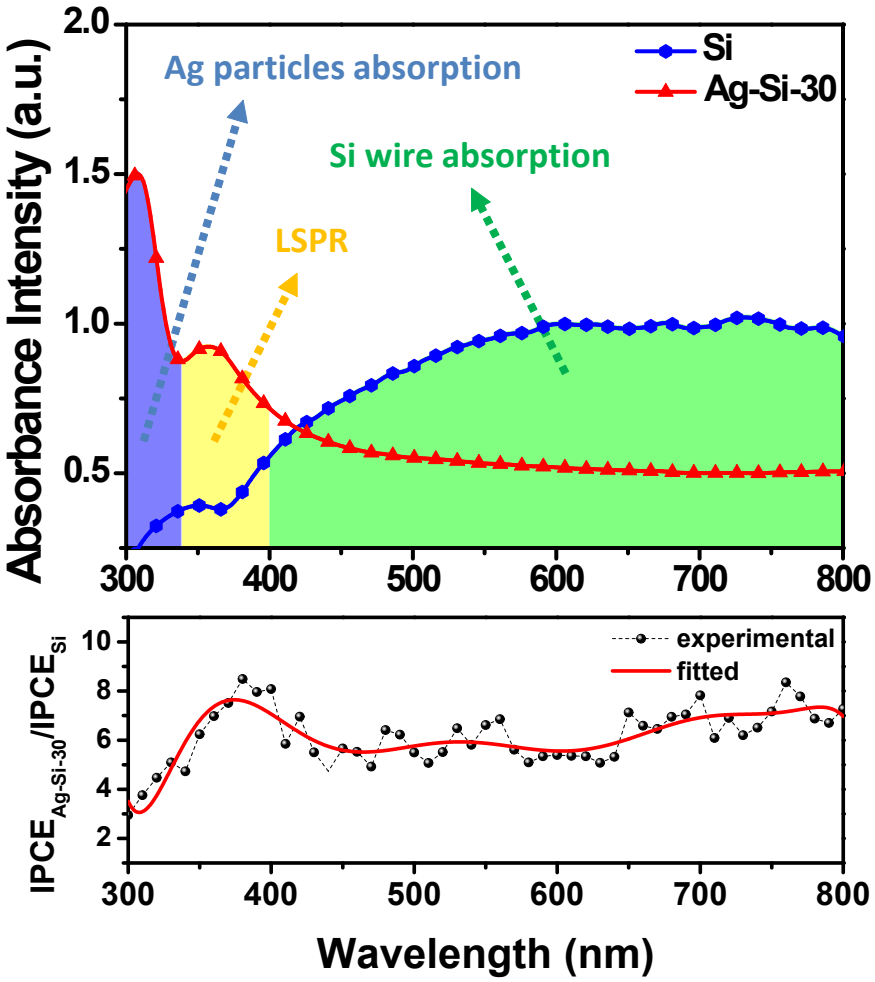

Figure S15. Absorption spectrum and IPCE enhancement of Ag-deposited Si MW array.